Total Internal Reflection with Fluorescence Correlation Spectroscopy: Combined Surface Reaction and Solution Diffusion

Tammy E. Starr and Nancy L. Thompson
Department of Chemistry, University of North Carolina, Chapel Hill, North Carolina 27599-3290 USA

ABSTRACT Total internal reflection with fluorescence correlation spectroscopy (TIR-FCS) is a method for measuring the surface association/dissociation rates and absolute densities of fluorescent molecules at the interface of solution and a planar substrate. This method can also report the apparent diffusion coefficient and absolute concentration of fluorescent molecules very close to the surface. An expression for the fluorescence fluctuation autocorrelation function in the absence of contributions from diffusion through the evanescent wave, in solution, has been published previously (N. L. Thompson, T. P. Burghardt, and D. Axelrod. 1981, *Biophys. J.* 33:435–454). This work describes the nature of the TIR-FCS autocorrelation function when both surface association/dissociation kinetics and diffusion through the evanescent wave contribute to the fluorescence fluctuations. The fluorescence fluctuation autocorrelation function depends in general on the kinetic association and dissociation rate constants, the surface site density, the concentration of fluorescent molecules in solution, the solution diffusion coefficient, and the depth of the evanescent field. Both general and approximate expressions are presented.

INTRODUCTION

A variety of biological processes are mediated by interactions between soluble ligands and cell surface receptors. Examples include immune processes that rely on interactions between soluble antibodies specific for pathogens and antibody receptors on immune cell surfaces (Daeron, 1997; Ravetch, 1997); neurological processes in which soluble transmitters such as serotonin stimulate cellular response by binding to specific receptors (Kim and Huganir, 1999; Seal and Amara, 1999); regulation of cellular growth and proliferation by interactions between specific growth factors and their cell-surface receptors (Hwa et al., 1999; Olofsson et al., 1999); and blood hemostasis, which is mediated in part by soluble proteins such as fibrinogen that associate with specific receptors on platelet surfaces (Clemetson and Clemetson, 1998; Zwaal et al., 1998).

One method for examining the thermodynamics and kinetics of ligand–receptor interactions is to use substrate-supported planar membranes (McConnell et al., 1986; Tamm and Kalb, 1993; Sackmann, 1996) and total internal reflection fluorescence microscopy (Axelrod, 1993; Thompson et al., 1993; Thompson and Lagerholm, 1997). In this approach, fluorescent ligands in solution interact with nonfluorescent receptors in the planar membranes. An excitation light source is internally reflected at the substrate/solution interface, creating a thin evanescent field that excites membrane-bound ligands (as well as those very close to the membrane). Measurement of the evanescently excited fluorescence as a function of the concentration of fluorescent ligands in solution yields binding curves from which equilibrium association constants may be measured (Pisarchick and Thompson, 1990; Hsieh et al., 1992). Information about surface association and dissociation kinetic rates may be found by using evanescent illumination with a concentration jump (Kalb et al., 1990; Müller et al., 1993) or with fluorescence photobleaching recovery (Hsieh and Thompson, 1995; Lagerholm et al., 2000).

A method similar to the combination of evanescent illumination with fluorescence photobleaching recovery is total internal reflection with fluorescence correlation spectroscopy (TIR-FCS) (Thompson et al., 1981; Thompson, 1982). In conventional fluorescence correlation spectroscopy (FCS), temporal fluctuations in the fluorescence measured from a small volume in solution are autocorrelated to provide information about the dynamics of the processes giving rise to the fluctuations (Elson and Magde, 1974; Magde et al., 1974; Palmer and Thompson, 1989a; Thompson, 1991). In TIR-FCS, the small observation volume is defined by using evanescent illumination and an aperture placed at an intermediate image plane of an optical microscope. The fluorescence measured from the small volume adjacent to the surface where internal reflection occurs fluctuates with time as individual fluorescent ligands diffuse into the volume, bind to surface-associated receptors, dissociate, and exit the volume. The fluorescence fluctuations are autocorrelated to obtain information about the association and dissociation rate constants for the ligand–receptor interaction. The experimental feasibility of TIR-FCS was initially demonstrated by examining the reversible, nonspecific adsorption of proteins to fused silica surfaces (Thompson and Axelrod, 1983), and this method has recently been used to examine the interaction of small molecules with chromatographic surfaces (Hansen and Harris, 1998a,b).

There has been considerable recent interest in developing FCS as a method for examining the properties of biochemical processes (e.g., Chen et al., 1999a, b; Korlach et al., 1999; Schuler et al., 1999; Vanden Broek et al., 1999;

Received for publication 26 July 2000 and in final form 4 December 2000.
Address reprint requests to Nancy L. Thompson, Department of Chemistry, CB #3290, University of North Carolina, Chapel Hill, NC 27599-3290. Tel.: 919-962-0328; Fax: 919-966-3675; E-mail: nlt@unc.edu.

0006-3495/01/03/1575/10 $2.00

Wiseman and Peterson, 1999; Bieschke et al., 2000; Cluzel et al., 2000; Schwille et al., 2000; Van Craenenbroeck and Engelborghs, 2000) and for use in high throughput screening (Sterrer and Henco, 1997; Auer et al., 1998; Fister et al., 1998; Silverman et al., 1998; Moore et al., 2000). A significant part of this effort has been directed toward detecting the reduction in the translational diffusion coefficient of a fluorescent ligand upon binding to a nonfluorescent receptor (e.g., Van Craenenbroeck and Engelborghs, 1999; Wohland et al., 1999). Although useful, this version of conventional solution-based FCS is limited for at least two reasons. First, translational diffusion is not very sensitive to size. Unless the receptor is considerably larger than the fluorescent ligand, the reduction in translational diffusion associated with receptor binding is not measurable (Meseth et al., 1999). Second, the average number of molecules in the illuminated volume must be small to produce fluorescence fluctuations of detectable magnitude, so the sample volume must be small. The resulting time for diffusion through the sample volume is usually in the millisecond range. Few ligand–receptor interactions of physiological interest have lifetimes on the order of, or shorter than, milliseconds. Therefore, the time dependence of the fluorescence fluctuation autocorrelation function contains information only about the equilibrium and not the kinetic aspects of the ligand–receptor interaction.

TIR-FCS autocorrelation functions depend directly on the kinetic rates describing the interaction of fluorescent ligands in solution with the surface binding sites (Thompson et al., 1981; Thompson, 1982). Thus, TIR-FCS may solve both major difficulties associated with using conventional solution-based FCS to monitor ligand–receptor interactions (low sensitivity to changes in translational diffusion and lack of direct information about kinetic rate constants). One aspect of TIR-FCS is that fluorescence fluctuations may arise not only from fluorescent ligands binding to and dissociating from surface-associated receptors, but also from ligand diffusion through the membrane-adjacent volume. Thus, there is a need for a theoretical expression that describes the manner in which solution diffusion and surface association/dissociation contribute to the measured autocorrelation function for samples in which both are significant. Such a theoretical expression would allow the two processes to be distinguished and the surface binding kinetics to be more accurately characterized. In addition, because FCS can be used in the microsecond time range, TIR-FCS has the ability to measure the apparent diffusion coefficient of fluorescent molecules very close to membrane surfaces. This effective diffusion coefficient is important in that it is expected to strongly affect the ligand–receptor kinetics. TIR-FCS also reports, in theory, the absolute density of surface-bound fluorescent ligands and the absolute concentration of fluorescent ligands close to the membrane surface. In this work, we present a comprehensive theory for TIR-FCS in which both surface kinetics and solution diffusion are significant. We demonstrate how one can extract from TIR-FCS autocorrelation functions the density of bound ligands, surface association and dissociation kinetic rates, and apparent diffusion coefficient and concentration of ligands very close to the membrane surface.

RESULTS

General considerations

Consider a reversible bimolecular reaction at a surface (the xy-plane) coupled with diffusion in solution ($z > 0$). A concentration of fluorescent molecules in solution, A, is in equilibrium with a density of fluorescent molecules on the surface, C, and a density of nonfluorescent, unoccupied surface binding sites, B (Fig. 1). The surface association and dissociation rate constants are k_a and k_d, respectively, and the equilibrium constant describing surface binding is $K = k_a/k_d = C/AB$. For a total density of surface binding sites S, $C = \beta KAS$ and $B = \beta S$ where $\beta = (1 + KA)^{-1}$ is the fraction of surface sites that are unoccupied at equilibrium. The fluorescent molecules diffuse in solution with coefficient D. In this work, we assume that both unoccupied (B) and occupied (C) surface binding sites are not translationally mobile along the surface.

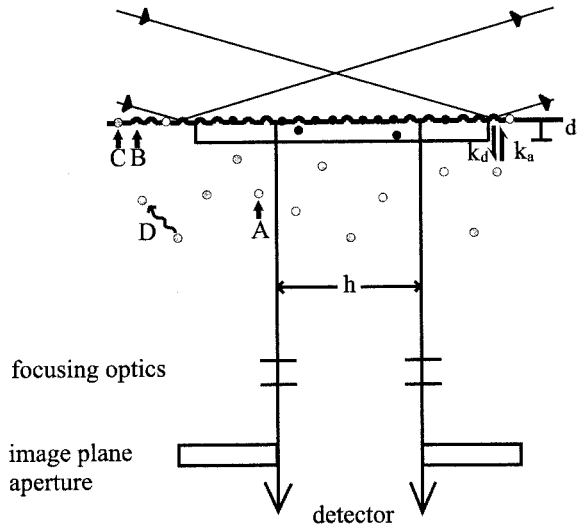

FIGURE 1 Schematic of TIR-FCS. Fluorescent molecules in solution, A, reversibly bind to free surface sites, B, forming complexes C. The association and dissociation kinetic rate constants are k_a and k_d, respectively. The diffusion coefficient of ligands in solution is D. Molecules bound or close to the surface are illuminated by an evanescent intensity of depth d. Fluorescence is measured from a surface area of h^2 through an aperture placed at an intermediate image plane. In this work, it is assumed that $h \gg d$ and that the surface binding sites and surface-bound complexes are not laterally mobile along the surface. Molecules fluoresce only when they are bound or close to the surface. Fluctuations in the measured fluorescence are autocorrelated. The fluorescence fluctuation autocorrelation function, $G(\tau)$, depends on k_a, k_d, A, D, d, and $S = B + C$.

The surface is illuminated by the evanescent field created by totally internally reflecting a laser beam at the surface/solution interface. The intensity of the evanescent field, I, decays exponentially as a function of the distance from the interface (Thompson et al., 1993). Thus, $I(z) = I_0 e^{-z/d}$ where I_0 is the evanescent intensity at the interface, and d is the evanescent depth. For fused silica and water, $d \approx 700$ Å (Lagerholm et al., 2000). Along with the evanescent field, a small aperture placed at an intermediate image plane of the microscope (of characteristic length h) defines an observation volume (Fig. 1).

At chemical equilibrium, individual molecules diffuse in solution within the observation volume; and bind to and dissociate from sites on the surface. These processes give rise to temporal fluctuations in the fluorescence measured from the observation volume. Of interest is the manner in which the autocorrelation function of these fluorescence fluctuations depends on the kinetic rates k_a and k_d, the surface site density S, the solution concentration A, the diffusion coefficient D, and the characteristic lengths d and h.

Definition of the fluorescence fluctuation autocorrelation function

The fluorescence measured from the observation volume, $F(t)$, is the sum of the fluorescence arising from surface-bound molecules, $F_C(t)$, and the fluorescence arising from molecules in solution, $F_A(t)$. The temporal fluorescence fluctuation is defined as the difference between the instantaneous fluorescence intensity and its average value; i.e., $\delta F(t) = F(t) - \langle F \rangle$, where the brackets denote an ensemble average. The normalized fluorescence fluctuation autocorrelation function is

$$G(\tau) = \frac{\langle \delta F(t+\tau)\delta F(t)\rangle}{\langle F\rangle^2} = \frac{\langle \delta F(\tau)\delta F(0)\rangle}{\langle F\rangle^2}, \qquad (1)$$

where the second equality holds for ergodic systems. Thus,

$$\begin{aligned} G(\tau) &= G_{CC}(\tau) + G_{CA}(\tau) + G_{AC}(\tau) + G_{AA}(\tau), \\ G_{CC}(\tau) &= \frac{\langle \delta F_C(\tau)\delta F_C(0)\rangle}{\langle F\rangle^2}, \\ G_{CA}(\tau) &= \frac{\langle \delta F_C(\tau)\delta F_A(0)\rangle}{\langle F\rangle^2}, \\ G_{AC}(\tau) &= \frac{\langle \delta F_A(\tau)\delta F_C(0)\rangle}{\langle F\rangle^2}, \\ G_{AA}(\tau) &= \frac{\langle \delta F_A(\tau)\delta F_A(0)\rangle}{\langle F\rangle^2}. \end{aligned} \qquad (2)$$

In Eq. 2, $\delta F_C(t) = F_C(t) - \langle F_C \rangle$, and $\delta F_A(t) = F_A(t) - \langle F_A \rangle$.

Approximate analytical expressions have been found for the efficiency of fluorescence collection through an aperture placed at an intermediate image plane (Koppel et al., 1976; Palmer and Thompson, 1989b). In this work, we assume that both the spatial dimension of the observed area in the x–y plane, h, and the depth of fluorescence collection efficiency along the z-axis are much larger than the evanescent wave depth, d. In this case,

$$\begin{aligned} F_C(t) &= QI_0 \int d^2r\, C(\mathbf{r}, t), \\ F_A(t) &= QI_0 \int d^2r \int_0^\infty dz\, e^{-z/d} A(\mathbf{r}, z, t), \end{aligned} \qquad (3)$$

where Q is a proportionality constant, $\mathbf{r} = (x, y)$ defines the surface/solution interface, and the limits of integration for dx and dy are from $-h/2$ to $h/2$. The temporally averaged fluorescence intensity is $\langle F \rangle = QI_0N$ where $N = N_C + N_A$ is the average number of fluorescent molecules in the observation volume. $N_C = Ch^2$ is the average number of fluorescent molecules on the surface within the observed area, and $N_A = Ah^2d$ is the average number of fluorescent molecules in solution within the observed volume.

Magnitude of the fluorescence fluctuation autocorrelation function

As described in the Appendix, $G_{CA}(0) = G_{AC}(0) = 0$ and

$$\begin{aligned} G(0) &= G_{CC}(0) + G_{AA}(0), \\ G_{CC}(0) &= \frac{\beta N_C}{(N_C + N_A)^2}, \quad G_{AA}(0) = \frac{N_A}{2(N_C + N_A)^2}. \end{aligned} \qquad (4)$$

In Eq. 4, β is the fraction of surface sites that are unoccupied at equilibrium as defined above.

When the average number of observed molecules in solution is much larger than the average number of observed molecules on the surface, $N_A \gg N_C$, and $G(0) \approx (2N_A)^{-1}$. When the average number of observed molecules on the surface is much larger than the average number of observed molecules in solution, $N_C \gg N_A$, and $G(0) \approx \beta N_C^{-1} + N_A(2N_C^2)^{-1}$. In this limit, the magnitude of the fluorescence fluctuation autocorrelation function may still depend on N_A; this behavior arises because fluctuations in the fluorescence arising from surface-bound molecules are very small when the surface is nearly saturated (see Appendix). $G(0)$ loses its dependence on N_A only if $\beta N_C \gg N_A$. In this case, $G(0) \approx \beta N_C^{-1}$.

The values of $G_{CC}(0)$ and $G_{AA}(0)$ may be rewritten as

$$\begin{aligned} G_{CC}(0) &= \frac{1}{N_S} \cdot \frac{\rho^2}{\alpha(1+\rho+\alpha)^2}, \\ G_{AA}(0) &= \frac{1}{N_S} \cdot \frac{\rho(1+\alpha)^2}{2\alpha(1+\rho+\alpha)^2} = \frac{1}{N_A} \cdot \frac{(1+\alpha)^2}{2(1+\rho+\alpha)^2}, \end{aligned} \qquad (5)$$

where $\alpha = KA$ is a normalized solution concentration and $\rho = KS/d$ describes the strength of surface binding relative to the evanescent depth d. $N_s = Sh^2$ is the total number of surface binding sites (occupied plus unoccupied) in the observed area. This number does not fluctuate with time. The fractions of the autocorrelation function amplitude arising from correlations in the density of surface-bound molecules, f_C, and in the concentration of molecules in solution, f_A, depend only on α and ρ:

$$f_C = \frac{G_{CC}(0)}{G(0)} = \frac{2\rho}{2\rho + (1+\alpha)^2},$$
$$f_A = \frac{G_{AA}(0)}{G(0)} = \frac{(1+\alpha)^2}{2\rho + (1+\alpha)^2}. \quad (6)$$

As shown in Fig. 2, the parameter ρ has a wide range of possible values (from 10^{-6} to 10^6) for typical values of K, S, and d. Therefore, the degree to which $G(0)$ reports information on the behavior of fluorescent molecules in solution or on the surface depends critically on the experimental conditions for which the data are obtained.

The dependence of $G(0)$ on α and ρ is shown in Fig. 3 along with the fractions of $G(0)$ that are associated with correlations in fluctuations of surface-bound molecules, f_C, and molecules in solution, f_A. When $2\rho \ll (1+\alpha)^2$, surface binding is weak, $f_A \approx 1$, and $G(0) = (2N_A)^{-1}$. In this limit, the system behaves as though surface binding is not present. When $2\rho \gg (1+\alpha)^2$, surface binding is strong, $f_C \approx 1$, and $G(0) \approx \beta N_C^{-1}$. In this limit, the system behaves as though evanescently excited molecules are not present in the solution. For a given average number of observed, surface-bound molecules, N_C, $G(0)$ is appreciable only far from saturation ($\beta \neq 0$) where the concentration fluctuations are more prominent.

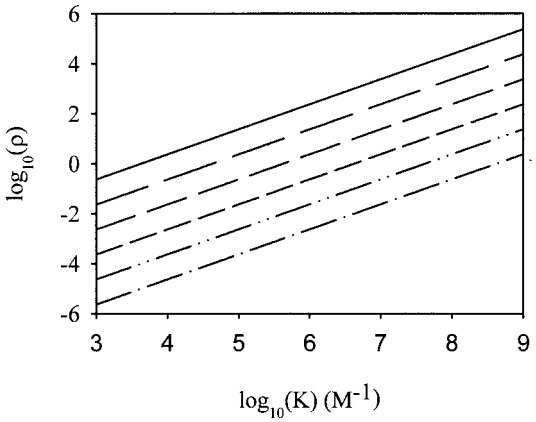

FIGURE 2 Typical values for the parameter ρ. The dimensionless parameter $\rho = (KS)/d$ describes the strength of the surface binding relative to the total surface site density S and the evanescent wave depth d. This plot shows the value of ρ as a function of the equilibrium surface association constant, for $10^3\ M^{-1} \leq K \leq 10^9\ M^{-1}$. The evanescent wave depth is 700 Å. The total surface site density S is (*line*) 10^4 molec/μm^2, (*long dash*) 10^3 molec/μm^2, (*intermediate dash*) 10^2 molec/μm^2, (*short dash*) 10 molec/μm^2, (*dash-dot-dot*) 1 molec/μm^2, and (*dash-dot*) 0.1 molec/μm^2.

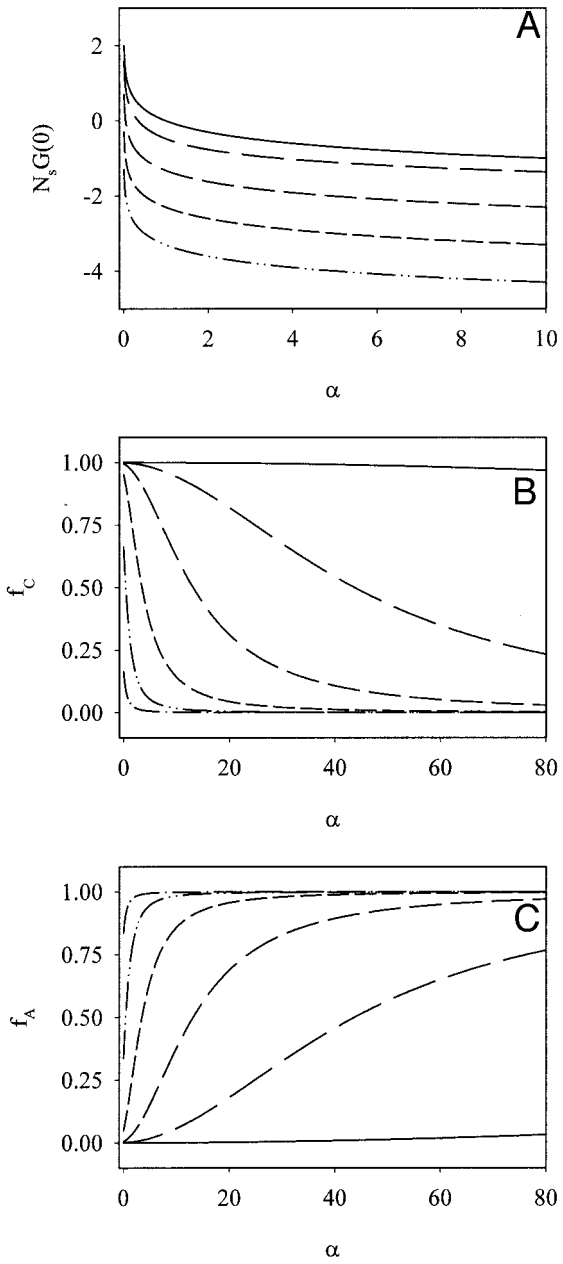

FIGURE 3 Magnitude of fluorescence fluctuation autocorrelation function $G(0)$. The manner in which (*A*) $N_S G(0)$, (*B*) f_C and (*C*) f_A depend on the normalized solution concentration α and the parameter ρ was calculated by using Eqs. 5 and 6. In (*A*), the parameter ρ is (*line*) 10^5, (*long dash*) 1, (*intermediate dash*) 0.1, (*short dash*) 0.01, and (*dash-dot-dot*) 10^{-3}. When $\alpha \rightarrow 0$, $G(0) \rightarrow \infty$. In (*B*) and (*C*), the parameter ρ is (*line*) 10^5, (*long dash*) 10^3, (*intermediate dash*) 100, (*short dash*) 10, (*dash-dot-dot*) 1, and (*dash-dot*) 0.1.

The solution concentration at which $G(0)$ contains equivalent fractions from surface-bound and solution molecules is determined by the condition that $f_A = f_C$, or $\alpha = (2\rho)^{1/2} - 1$. At solution concentrations below this value, $G(0)$ reports

information primarily about surface association and dissociation kinetics. At solution concentrations above this value, $G(0)$ reports information primarily about diffusion in solution. Therefore, it is theoretically possible to increase the solution concentration to a point where $G(0)$ primarily reflects the diffusional behavior of molecules in solution but very close to the surface. However, for weak surface binding, it may not be possible to decrease the solution concentration far enough so that $G(0)$ primarily reflects surface association and dissociation kinetics. The parameter f_C can be made appreciable by lowering the solution concentration only for values of $\rho \geq 1$. For $d = 700$ Å and $S = 1000$ molec/μm^2, this conditions corresponds to $K \geq 4 \times 10^4$ M^{-1} (Fig. 2).

General solution for the fluorescence fluctuation autocorrelation function

As described in the Appendix, the fluorescence fluctuation autocorrelation function is given by

$$\frac{G(\tau)}{G(0)} = g_1 w[-i(R_1\tau)^{1/2}] + g_2 w[-i(R_2\tau)^{1/2}] + g_3 w[i(R_e\tau)^{1/2}] + g_4\left\{\left(\frac{R_e\tau}{\pi}\right)^{1/2} - R_e\tau w[i(R_e\tau)^{1/2}]\right\}, \quad (7)$$

where $G(0)$ is given by the expressions in Eqs. 4 and 5. The shape of $G(\tau)$ is determined by monotonically decaying w-functions, which are defined as (Abramowitz and Stegun, 1974)

$$w(\xi) = e^{-\xi^2}\mathrm{erfc}(-i\xi). \quad (8)$$

The amplitudes are

$$g_{1,2} = \pm\frac{f_C}{R_1^{1/2} - R_2^{1/2}}\left[R_{1,2}^{1/2} + R_r\left(\frac{1}{R_t^{1/2}} + \frac{2}{R_{3,4}^{1/2}} - \frac{R_{1,2}^{1/2}}{R_{3,4}}\right)\right],$$
$$g_3 = f_A + \frac{f_C R_r}{(R_3R_4)^{1/2}}\left[2 + \frac{R_e - R_r}{(R_3R_4)^{1/2}}\right], \quad (9)$$
$$g_4 = 2\left[f_A + \frac{f_C R_r}{(R_3R_4)^{1/2}}\right],$$

and the rates are

$$R_{3,4}^{1/2} = R_{1,2}^{1/2} + R_e^{1/2},$$
$$R_{1,2}^{1/2} = -\frac{R_r}{2R_t^{1/2}} \pm \left(\frac{R_r^2}{4R_t} - R_r\right)^{1/2}, \quad (10)$$

where

$$R_r = k_a A + k_d, \quad R_t = D\left(\frac{A}{\beta C}\right)^2, \quad R_e = \frac{D}{d^2}. \quad (11)$$

The three fundamental rates that determine $G(\tau)$ are R_r, R_t, and R_e (Eq. 11). R_r is the relaxation rate for a pseudo first-order reaction and increases with the solution concentration of fluorescent molecules, A. By measuring R_r as a function of A, the intrinsic association and dissociation kinetic rates for the surface reaction may be found. R_t is a rate describing transport in solution through the distance $\beta C/A = KS\beta^2$. As described previously, the relative values of R_r and R_t determine the extent to which previously dissociated molecules rebind to the surface (Thompson et al., 1981; Lagerholm and Thompson, 1998, 2000). R_e is the rate for diffusion through the depth of the evanescent intensity. $G(\tau)$ is shown in Fig. 4 for a typical set of experimental parameters.

Limit of no molecules in solution

When the molecules bind tightly to the surface, $2\rho \gg (1 + \alpha)^2$ and $f_A \ll f_C$. This condition is mathematically equivalent to the statement that $R_e \gg R_t$. If, in addition, $R_e \gg R_r$,

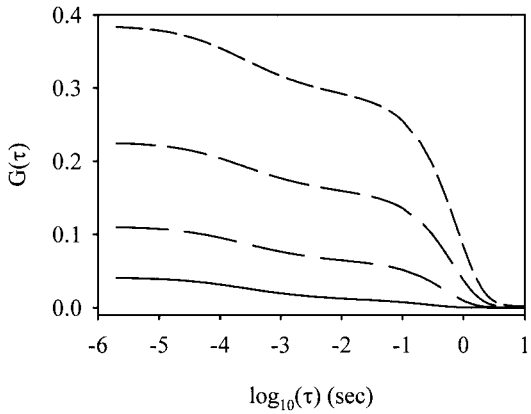

FIGURE 4 Fluorescence fluctuation autocorrelation function $G(\tau)$. $G(\tau)$ was calculated from Eqs. 7–11 and is shown for $k_a = 10^7$ M^{-1}sec^{-1}, $k_d = 1$ sec^{-1}, $S = 10$ molec/μm^2, $d = 700$ Å, $h = 0.7$ μm, and $D = 5 \times 10^{-7}$ cm^{2}sec^{-1}. For these conditions, $R_e = 1.0 \times 10^4$ sec^{-1}. $G(\tau)$ is shown for the following solution concentrations and consequent rates: *line*, $A = 0.3$ μM, $R_r = 4$ sec^{-1}, $R_t = 4.6 \times 10^5$ sec^{-1}; *long dash*, $A = 0.1$ μM, $R_r = 2$ sec^{-1}, $R_t = 2.9 \times 10^4$ sec^{-1}; *intermediate dash*, $A = 0.05$ μM, $R_r = 1.5$ sec^{-1}, $R_t = 9.2 \times 10^3$ sec^{-1}; and *short dash*, $A = 0.03$ μM, $R_r = 1.3$ sec^{-1}, $R_t = 5.1 \times 10^3$ sec^{-1}. At short times, $G(\tau)$ decays primarily by diffusion of the fluorescent molecules in solution through the depth of the evanescent intensity. At longer times, the decay of $G(\tau)$ reflects the surface binding kinetics and, for the curves shown here, depends primarily on the rate R_r because $R_r \ll R_t$. The length $KS = 1660$ Å, the parameter $\rho = 2.4$, and $0.3 \leq \alpha \leq 3$. Therefore, at the lowest solution concentration (*short dash*), the fractions of $G(0)$ arising from solution diffusion and from surface binding kinetics are $f_A = 0.26$ and $f_C = 0.74$. At the highest solution concentration (*line*), these fractions are $f_A = 0.77$ and $f_C = 0.23$ (Eq. 6). The values of $G(\tau)$ are equivalent within plot resolution to the more simple, approximate expression given in Eq. 16. The half-times decrease with the solution concentration from 0.30 sec ($A = 0.03$ μM) to 0.88 msec ($A = 0.3$ μM).

then $g_3 = g_4 = 0$ and

$$G(\tau) = \frac{1}{N_S} \cdot \frac{1}{KA} \cdot \frac{R_1^{1/2} w[-i(R_2\tau)^{1/2}] - R_2^{1/2} w[-i(R_1\tau)^{1/2}]}{R_1^{1/2} - R_2^{1/2}}. \quad (12)$$

This function has been described previously (Thompson et al., 1981; Lagerholm and Thompson, 1998; Lagerholm et al., 2000) and is shown in Fig. 5. When the reaction rate R_r is much less than the transport rate R_t, $R_{1,2}^{1/2} \approx \pm R_r^{1/2}$ (Eq. 10) and (Abramowitz and Stegun, 1974)

$$G(\tau) = \frac{1}{N_S} \cdot \frac{1}{KA} \cdot \exp[-(k_a A + k_d)\tau]. \quad (13)$$

When the transport rate R_t is much less than the reaction rate R_r, $R_1^{1/2} \approx -R_t^{1/2}$, $R_2^{1/2} \approx -R_r/R_t^{1/2}$, $R_2^{1/2} \gg R_1^{1/2}$, and

$$G(\tau) = \frac{1}{N_S} \cdot \frac{1}{KA} \cdot w\left[i(1 + KA)^2 \frac{(D\tau)^{1/2}}{KS} \right]. \quad (14)$$

The ratio R_t/R_r increases with the solution concentration A (Eq. 11). Therefore, as this concentration is increased, $G(\tau)$ proceeds from the shape shown in Eq. 14 to that shown in Eq. 13. However, the simple limit of Eq. 13 can be reached by increasing A only if the surface binding is tight enough so that both $R_t \gg R_r$ and $2\rho \gg (1 + \alpha)^2$.

Limit of no surface binding

When the molecules do not bind to the surface, $\rho = f_C = 0$. This equality implies that $G_{CC}(\tau) = G_{CA}(\tau) = G_{AC}(\tau) = 0$ (Appendix). From Eqs. 7 and 9 with $f_C = 0$,

$$G(\tau) = \frac{1}{2N_A} \left\{ (1 - 2R_e\tau) w[i(R_e\tau)^{1/2}] + 2\left(\frac{R_e\tau}{\pi}\right)^{1/2} \right\}. \quad (15)$$

As shown in Fig. 6, this function decays monotonically with τ from $(2N_A)^{-1}$ to zero. The characteristic decay time is R_e^{-1} and the ratio of the initial slope to the initial value is $-R_e$.

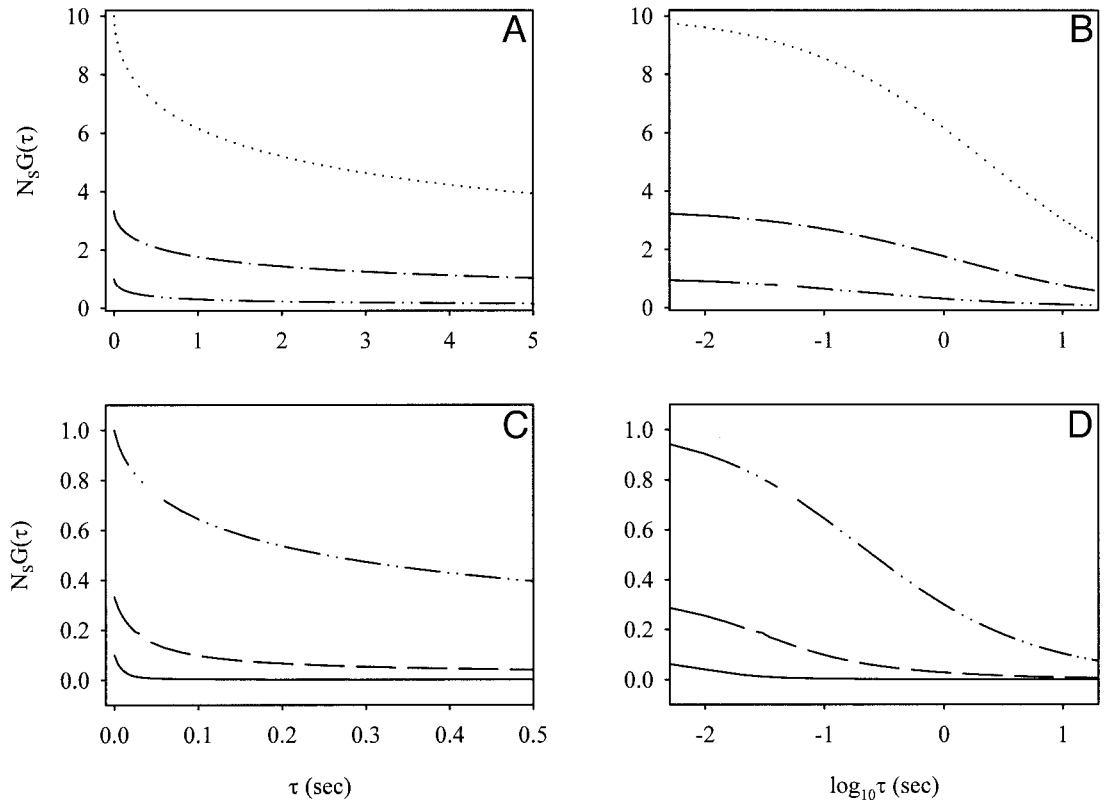

FIGURE 5 $G(\tau)$ in the limit of no molecules in solution. $N_S G(\tau)$ was calculated by using Eqs. 10–12. In these plots, $k_a = 10^8$ $M^{-1}sec^{-1}$, $k_d = 10$ sec^{-1}, $S = 10^3$ molec/μm^2, and $D = 5 \times 10^{-7}$ cm^2sec^{-1}. The solution concentration A is (*line*) 1 μM, (*dash*) 0.3 μM, (*dash-dot-dot*) 0.1 μM, (*dash-dot*) 0.03 μM, and (*dot*) 0.01 μM. At the lowest solution concentration, $R_r = 11$ sec^{-1}, $R_t = 0.27$ sec^{-1}, and $G(\tau)$ is nearly identical to Eq. 14 for $A = 0.01$ μM (not shown). At the highest solution concentration, $R_r = 110$ sec^{-1}, $R_t = 2700$ sec^{-1}, and $G(\tau)$ is nearly identical to Eq. 13 for $A = 1$ μM (not shown). The length KS is 1.66×10^{-3} cm and, for an evanescent wave depth d equal to 700 Å, the parameter ρ is 240. Therefore, $2\rho \gg (1 + \alpha)^2$ for most curves and contributions from molecules diffusing in solution within the depth of the evanescent intensity are small. The half-times decrease with the solution concentration from 2.3 sec ($A = 0.01$ μM) to 6.3 msec ($A = 1$ μM).

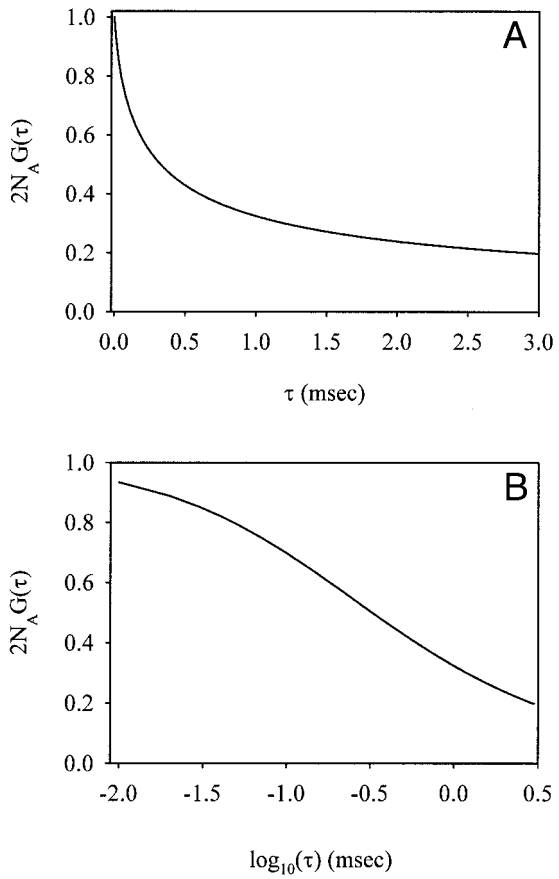

FIGURE 6 $G(\tau)$ in the limit of no surface binding. $2N_A G(\tau)$ was calculated by using Eq. 15 with $R_e = 1.02 \times 10^4$ sec^{-1}. This function decays monotonically with time. The time where $G(\tau)$ has decreased to one-half of its initial value is 3.3 R_e^{-1}. The ratio of the initial slope and the initial value is $-R_e$.

Approximate expression for $G(\tau)$

In most experimental systems of interest, $R_r \ll R_e$. In this case, $G(\tau)$ is a weighted sum of the limits shown in Eqs. 12 and 15:

$$G(\tau) = \left\{\frac{R_1^{1/2} w[-i(R_2\tau)^{1/2}] - R_2^{1/2} w[-i(R_1\tau)^{1/2}]}{R_1^{1/2} - R_2^{1/2}}\right\} G_{CC}(0) + \left\{(1 - 2R_e\tau) w[i(R_e\tau)^{1/2}] + 2\left(\frac{R_e\tau}{\pi}\right)^{1/2}\right\} G_{AA}(0), \quad (16)$$

where $G_{CC}(0)$ and $G_{AA}(0)$ are given by Eqs. 4 and 5. For many experimental conditions, Eq. 16 will be adequate. The values of $G(\tau)$ calculated from Eqs. 7 and 16 are compared in Fig. 4.

DISCUSSION

FCS is of growing importance as a method for characterizing interaction dynamics in biochemical systems (e.g., Chen et al., 1999a b; Korlach et al., 1999; Schuler et al., 1999; Winkler et al., 1999; Wiseman and Peterson, 1999; Vanden Broek et al., 1999; Van Craenenbroeck and Engelborghs, 2000; Bieschke et al., 2000; Cluzel et al., 2000; Moore et al., 2000; Schwille et al., 2000). This technique is also of considerable current interest to the pharmaceutical community in that it has significant potential as a method for high throughput screening of drug–target interactions (Sterrer and Henco, 1997; Auer et al., 1998; Fister et al., 1998; Silverman et al., 1998; Moore et al., 2000). One limitation of the most common form of solution-based FCS is that information is obtained only about the equilibrium and not the kinetic parameters governing the biochemical interactions that are examined (e.g., Van Craenenbroeck and Engelborghs, 1999; Wohland et al., 1999). As described in this work, one method of overcoming this limitation is to use TIR-FCS, which yields direct information about the association and dissociation kinetic rate constants. This technique is not limited to the interaction of fluorescent ligands with membrane-bound receptors, but might also be used to study a variety of protein–protein interactions in that a number of methods have been developed for immobilizing functional, soluble proteins on transparent surfaces. In addition, as described here, TIR-FCS can monitor the diffusion coefficients and concentrations of fluorescent ligands very close to membrane surfaces.

In previous work, a theory was developed for the interpretation of TIR-FCS autocorrelation functions arising solely from the association and dissociation of fluorescent ligands with surface binding sites (Thompson et al., 1981; Thompson, 1982). In this case, the magnitude of the fluorescence fluctuation autocorrelation function reports the density of surface-bound ligands and the temporal decay depends on the intrinsic relaxation rate for the interaction, R_r, and a rate describing transport in solution, R_t (Eq. 11). In this work, we have presented a more general expression for the TIR-FCS autocorrelation function, which is applicable to situations in which both surface kinetics and diffusion through the depth of the evanescent field contribute to the fluorescence fluctuations (Eqs. 7–9; Fig. 4). This more general expression depends on R_r, R_t, and an additional rate, R_e, which describes diffusion through the evanescent wave depth (Eq. 11). The general expression reduces to the previously published form in the absence of fluctuations from diffusion through the evanescent wave depth (Eqs. 12–14; Fig. 5) and to a simple expression in the absence of fluctuations from surface reaction (Eq. 15; Fig. 6). For most systems of biochemical interest, the rate of diffusion through the evanescent field (R_e) will be much more rapid than the rates describing the surface reaction (R_r and R_t). In this case, the general expression for $G(\tau)$ (Eqs. 7–9) can be approximated by a weighted sum of the two more simple expressions (Eq. 16; Fig. 4).

APPENDIX: DERIVATION OF THE FLUORESCENCE FLUCTUATION AUTOCORRELATION FUNCTION

Definition of the normalized fluorescence fluctuation autocorrelation function

The concentration fluctuations as a function of position and time are $\delta C(\mathbf{r}, t) = C(\mathbf{r}, t) - \langle C\rangle$ and $\delta A(\mathbf{r}, z, t) = A(\mathbf{r}, z, t) - \langle A\rangle$. By using these expressions in Eqs. 1–3, one finds that

$$G_{CC}(\tau) = \frac{1}{N^2}\int d^2r \int d^2r' \phi_{CC}(\mathbf{r}, \mathbf{r}', \tau),$$

$$G_{AC}(\tau) = \frac{1}{N^2}\int d^2r \int d^2r' \int_0^\infty dz e^{-z/d}\phi_{AC}(\mathbf{r}, \mathbf{r}', z, \tau),$$

$$G_{CA}(\tau) = \frac{1}{N^2}\int d^2r \int d^2r' \int_0^\infty dz' e^{-z'/d}\phi_{CA}(\mathbf{r}, \mathbf{r}', z', \tau),$$

$$G_{AA}(\tau) = \frac{1}{N^2}\int d^2r \int d^2r' \int_0^\infty dz \int_0^\infty dz' e^{-z/d}e^{-z'/d}\phi_{AA}(\mathbf{r}, \mathbf{r}', z, z', \tau), \quad \text{(A1)}$$

where N is the average number of fluorescent molecules in the observation volume (see text) and

$$\begin{aligned}\phi_{CC}(\mathbf{r}, \mathbf{r}', \tau) &= \langle \delta C(\mathbf{r}, \tau)\delta C(\mathbf{r}', 0)\rangle,\\ \phi_{AC}(\mathbf{r}, \mathbf{r}', z, \tau) &= \langle \delta A(\mathbf{r}, z, \tau)\delta C(\mathbf{r}', 0)\rangle,\\ \phi_{CA}(\mathbf{r}, \mathbf{r}', z', \tau) &= \langle \delta C(\mathbf{r}, \tau)\delta A(\mathbf{r}', z', 0)\rangle,\\ \phi_{AA}(\mathbf{r}, \mathbf{r}', z, z', \tau)\rangle &= \langle \delta A(\mathbf{r}, z, \tau)\delta A(\mathbf{r}', z', 0)\rangle.\end{aligned} \quad \text{(A2)}$$

The functions ϕ are autocorrelations and cross-correlations of fluctuations in the solution concentration and surface density of fluorescent molecules.

Magnitude of the fluorescence fluctuation autocorrelation function

The magnitude of $G(\tau)$ is found by evaluating Eqs. A1 at $\tau = 0$. The initial values of the concentration fluctuation correlation functions are (Elson and Magde, 1974; Thompson et al., 1981)

$$\begin{aligned}\phi_{CC}(\mathbf{r}, \mathbf{r}', 0) &= \beta C\delta(\mathbf{r} - \mathbf{r}'),\\ \phi_{AC}(\mathbf{r}, \mathbf{r}', z, 0) &= \phi_{CA}(\mathbf{r}, \mathbf{r}', z', 0) = 0,\\ \phi_{AA}(\mathbf{r}, \mathbf{r}', z, z', 0) &= A\delta(\mathbf{r} - \mathbf{r}')\delta(z - z'),\end{aligned} \quad \text{(A3)}$$

where β is the fraction of surface binding sites that is free at equilibrium (see text). Fluctuations in the concentrations of molecules of different species (free in solution, A, and surface-bound, C) are not correlated at the same time. Molecules diffusing through the open, illuminated volume (A) are correlated at the same time only at the same place. This result is also the case for molecules bound to the surface (C), but the magnitude of the correlation is reduced by the factor β. By using Eqs. A3 in Eqs. A1, one finds that $G_{AC}(0) = G_{CA}(0) = 0$ and Eqs. 4.

Differential equations and boundary conditions

For most experimental situations, the evanescent depth d is at least ten-fold smaller than the characteristic length of the observation area h. In this case, the differential equations describing combined surface reaction and solution diffusion are (Thompson et al., 1981; Lagerholm and Thompson, 1998)

$$\begin{aligned}\frac{\partial}{\partial t}C(\mathbf{r}, t) &= k_a B(\mathbf{r}, t)[A(\mathbf{r}, z, t)]_{z=0} - k_d C(\mathbf{r}, t),\\ \frac{\partial}{\partial t}A(\mathbf{r}, z, t) &= D\frac{\partial^2}{\partial z^2}A(\mathbf{r}, z, t).\end{aligned} \quad \text{(A4)}$$

By using the expressions for $\delta C(\mathbf{r}, t)$ and $\delta A(\mathbf{r}, z, t)$ from above in Eq. A4, neglecting the term proportional to $\delta C(\mathbf{r}, t)\delta A(\mathbf{r}, z, t)$, and noting that $\delta B(\mathbf{r}, t) = -\delta C(\mathbf{r}, t)$ because S does not fluctuate with time, one finds that

$$\begin{aligned}\frac{\partial}{\partial t}\delta C(\mathbf{r}, t) &= k_a B[\delta A(\mathbf{r}, z, t)]_{z=0} - R_r\delta C(\mathbf{r}, t),\\ \frac{\partial}{\partial t}\delta A(\mathbf{r}, z, t) &= D\frac{\partial^2}{\partial z^2}\delta A(\mathbf{r}, z, t),\end{aligned} \quad \text{(A5)}$$

where R_r is the primary relaxation rate for the surface reaction (Eq. 11). Multiplying Eqs. A5 by either $\delta C(\mathbf{r}', 0)$ or $\delta A(\mathbf{r}', z', 0)$ and taking ensemble averages yields

$$\begin{aligned}\frac{\partial}{\partial \tau}\phi_{CC}(\mathbf{r}, \mathbf{r}', \tau) &= k_a B[\phi_{AC}(\mathbf{r}, \mathbf{r}', z, \tau)]_{z=0} - R_r\phi_{CC}(\mathbf{r}, \mathbf{r}', \tau),\\ \frac{\partial}{\partial \tau}\phi_{CA}(\mathbf{r}, \mathbf{r}', z', \tau) &= k_a B[\phi_{AA}(\mathbf{r}, \mathbf{r}', z, z', \tau)]_{z=0} - R_r\phi_{CA}(\mathbf{r}, \mathbf{r}', z', \tau),\\ \frac{\partial}{\partial \tau}\phi_{AC}(\mathbf{r}, \mathbf{r}', z, \tau) &= D\frac{\partial^2}{\partial z^2}\phi_{AC}(\mathbf{r}, \mathbf{r}', z, \tau),\\ \frac{\partial}{\partial \tau}\phi_{AA}(\mathbf{r}, \mathbf{r}', z, z', \tau) &= D\frac{\partial^2}{\partial z^2}\phi_{AA}(\mathbf{r}, \mathbf{r}', z, z', \tau).\end{aligned} \quad \text{(A6)}$$

Two of the four required boundary conditions are

$$[\phi_{AC}(\mathbf{r}, \mathbf{r}', z, \tau)]_{z=\infty} = [\phi_{AA}(\mathbf{r}, \mathbf{r}', z, z', \tau)]_{z=\infty} = 0. \quad \text{(A7)}$$

The remaining two boundary conditions are found from the condition describing the flux at the surface,

$$D\left[\frac{\partial}{\partial z}A(\mathbf{r}, z, \tau)\right]_{z=0} = k_a B(\mathbf{r}, \tau)[A(\mathbf{r}, z, \tau)]_{z=0} - k_d C(\mathbf{r}, \tau), \quad \text{(A8)}$$

or

$$D\left[\frac{\partial}{\partial z}\,\phi_{AC}(\mathbf{r}, \mathbf{r}', z, \tau)\right]_{z=0} = k_a B[\phi_{AC}(\mathbf{r}, \mathbf{r}', z, \tau)]_{z=0} - R_r\phi_{CC}(\mathbf{r}, \mathbf{r}', \tau). \quad \text{(A9)}$$

$$D\left[\frac{\partial}{\partial z}\,\phi_{AA}(\mathbf{r}, \mathbf{r}', z, z', \tau)\right]_{z=0} = k_a B[\phi_{AA}(\mathbf{r}, \mathbf{r}', z, z', \tau)]_{z=0} - R_r\phi_{CA}(\mathbf{r}, \mathbf{r}', z', \tau).$$

Concentration fluctuation autocorrelation and cross-correlation functions

The concentration fluctuation correlation functions may be found by using Laplace transforms as previously described (Thompson et al., 1981; Hsieh and Thompson, 1994; Lagerholm and Thompson, 1998). The results are

$$\phi_{CC}(\mathbf{r}, \mathbf{r}', \tau) = \frac{\beta C\delta(\mathbf{r} - \mathbf{r}')}{R_1^{1/2} - R_2^{1/2}} \cdot \{R_1^{1/2} w[-i(R_2\tau)^{1/2}] - R_2^{1/2} w[-i(R_1\tau)^{1/2}]\},$$

$$\phi_{CA}(\mathbf{r}, \mathbf{r}', z, \tau) = \phi_{AC}(\mathbf{r}, \mathbf{r}', z, \tau) = \frac{k_d C\delta(\mathbf{r} - \mathbf{r}')}{D^{1/2}(R_1^{1/2} - R_2^{1/2})} \cdot e^{-z^2/4D\tau} \cdot \left\{ w\left[\frac{iz}{(4D\tau)^{1/2}} - i(R_1\tau)^{1/2}\right] - w\left[\frac{iz}{(4D\tau)^{1/2}} - i(R_2\tau)^{1/2}\right]\right\},$$

$$\phi_{AA}(\mathbf{r}, \mathbf{r}', z, ' \tau) = \frac{A\delta(\mathbf{r} - \mathbf{r}')}{(4\pi D\tau)^{1/2}} \cdot \{e^{-(z-z')^2/4D\tau} + e^{-(z+z')^2/4D\tau}\} - \frac{k_d C\delta(\mathbf{r} - \mathbf{r}')}{D(R_1^{1/2} - R_2^{1/2})} \cdot \left\{ R_1^{1/2} e^{-(z+z')^2/4D\tau} w\left[\frac{i(z + z')}{(4D\tau)^{1/2}} - i(R_1\tau)^{1/2}\right] - R_2^{1/2} e^{-(z+z')^2/4D\tau} w\left[\frac{i(z + z')}{(4D\tau)^{1/2}} - i(R_2\tau)^{1/2}\right]\right\}. \quad \text{(A10)}$$

Rates R_1 and R_2 are defined in Eqs. 10.

Normalized fluorescence fluctuation autocorrelation function

The fluorescence fluctuation autocorrelation function $G(\tau)$ may be found by using Eqs. A10 in Eqs. A1. Completing the integrals (Abramowitz and Stegun, 1974) yields

$$\frac{G_{CC}(\tau)}{G(0)} = \frac{f_C}{R_1^{1/2} - R_2^{1/2}} \{R_1^{1/2} w[-i(R_2\tau)^{1/2}] - R_2^{1/2} w[-i(R_1\tau)^{1/2}]\}, \quad \text{(A11)}$$

$$\frac{G_{CA}(\tau)}{G(0)} = \frac{G_{AC}(\tau)}{G(0)} = \frac{f_C R_r}{R_1^{1/2} - R_2^{1/2}} \left\{\frac{w[-i(R_1\tau)^{1/2}]}{R_3^{1/2}} - \frac{w[-i(R_2\tau)^{1/2}]}{R_4^{1/2}} + \left(\frac{1}{R_4^{1/2}} - \frac{1}{R_3^{1/2}}\right) w[i(R_e\tau)^{1/2}]\right\}, \quad \text{(A12)}$$

$$\frac{G_{AA}(\tau)}{G(0)} = \frac{f_C R_r}{R_1^{1/2} - R_2^{1/2}} \left\{\frac{R_2^{1/2}}{R_4} w[-i(R_2\tau)^{1/2}] - \frac{R_1^{1/2}}{R_3} w[-i(R_1\tau)^{1/2}]\right\} + 2\left[f_A + \frac{f_C R_r}{(R_3R_4)^{1/2}}\right]\left(\frac{R_e\tau}{\pi}\right)^{1/2} + \left\{\left[f_A + \frac{f_C R_r(R_e - R_r)}{R_3R_4}\right] - 2\left[f_A + \frac{f_C R_r}{(R_3R_4)^{1/2}}\right] R_e\tau\right\} w[i(R_e\tau)^{1/2}, \quad \text{(A13)}$$

where the rates R_3 and R_4 are given in Eqs. 10 and the fractions f_A and f_C are given in Eq. 6. Summing the terms in Eqs. A11–A13 gives Eqs. 7 and 9.

We thank Daniel Axelrod for helpful conversations. This work was supported by NSF Grant MCB-9728116 and North Carolina Biotechnology Center Grant 2000-ARG-0026.

REFERENCES

Abramowitz, M., and I. A. Stegun. 1974. Handbook of Mathematical Functions. Dover Publications, New York. 297–329.

Auer, M., K. J. Moore, F. J. Meyer-Almes, R. Guenther, A. J. Pope, and K. A. Stoeckli. 1998. Fluorescence correlation spectroscopy: lead discovery by miniaturized HTS. *Drug Discov. Today.* 3:457–465.

Axelrod, D. 1993. Total internal reflection fluorescence microscopy. *Methods Cell Biol.* 30:245–270.

Bieschke, J., A. Giese, W. Schulz-Schaeffer, I. Zerr, S. Poser, M. Eigen, and H. Kretzschmar. 2000. Ultrasensitive detection of pathological prion protein aggregates by dual-color scanning for intensely fluorescent targets. *Proc. Natl. Acad. Sci. USA.* 97:5468–5473.

Chen, Y., J. D. Muller, P. T. C. So, and E. Gratton. 1999a. The photon counting histogram in fluorescence fluctuation spectroscopy. *Biophys. J.* 77:553–567.

Chen, Y., J. D. Muller, K. M. Berland, and E. Gratton. 1999b. Fluorescence fluctuation spectroscopy. *Methods Companion to Meth. Enzymol.* 19: 234–252.

Clemetson, K. J., and J. M. Clemetson. 1998. Integrins and cardiovascular disease. *Cell. Mol. Life Sci.* 54:502–513.

Cluzel, P., M. Surette, and S. Leibler. 2000. An ultrasensitive bacterial motor revealed by monitoring signaling proteins in single cells. *Science.* 287:1652–1655.

Daeron, M. 1997. Fc receptor biology. *Annu. Rev. Immunol.* 15:203–234.

Elson, E. L., and D. Magde. 1974. Fluorescence correlation spectroscopy. I. Conceptual basis and theory. *Biopolymers.* 13:1–27.

Fister, J. C., S. C. Jacobson, L. M. Davis, and J. M. Ramsey. 1998. Counting single chromophore molecules for ultrasensitive analysis and separations on microchip devices. *Anal. Chem.* 70:431–437.

Hansen, R. L., and J. M. Harris. 1998a. Total internal reflection fluorescence correlation spectroscopy for counting molecules at solid/liquid interfaces. *Analy. Chem.* 70:2565–2575.

Hansen, R. L., and J. M. Harris. 1998b. Measuring reversible adsorption kinetics of small molecules at solid/liquid interfaces by total internal reflection fluorescence correlation spectroscopy. *Anal. Chem.* 70: 4247–4256.

Hsieh, H. V., C. L. Poglitsch, and N. L. Thompson. 1992. Direct measurement of the weak interactions between a mouse Fc receptor (FcγRII) and IgG1 in the absence and presence of hapten: a total internal reflection fluorescence microscopy study. *Biochemistry.* 31:11562–11566.

Hsieh, H. V., and N. L. Thompson. 1994. Theory for measuring bivalent surface binding kinetics using total internal reflection with fluorescence photobleaching recovery. *Biophys. J.* 66:898–911.

Hsieh, H. V., and N. L. Thompson. 1995. Dissociation kinetics between a mouse Fc receptor (FcγRII) and IgG: measurement by total internal reflection with fluorescence photobleaching recovery. *Biochemistry.* 34: 12481–12488.

Hwa, V., Y. Oh, and R. G. Rosenfeld. 1999. The insulin-like growth factor-binding protein (IGFBP) superfamily. *Endocrine Rev.* 20: 761–787.

Kalb, E., J. Engel, and L. K. Tamm. 1990. Binding of proteins to specific target sites in membranes measured by total internal reflection fluorescence microscopy. *Biochemistry.* 29:1607–1613.

Kim, J. H., and R. L. Huganir. 1999. Organization and regulation of proteins at synapses. *Curr. Opin. Cell Biol.* 11:248–254.

Koppel, D. E., D. Axelrod, J. Schlessinger, E. L. Elson, and W. W. Webb. 1976. Dynamics of fluorescence marker concentration as a probe of mobility. *Biophys. J.* 16:1315–1329.

Korlach, J., P. Schwille, W. W. Webb, and G. W. Feigenson. 1999. Characterization of lipid bilayer phases by confocal microscopy and fluorescence correlation spectroscopy. *Proc. Natl. Acad. Sci. USA.* 96: 8461–8466.

Lagerholm, B. C., and N. L. Thompson. 1998. Theory for ligand rebinding at cell membrane surfaces. *Biophys. J.* 74:1215–1228.

Lagerholm, B. C., and N. L. Thompson. 2000. Temporal dependence of ligand dissociation and rebinding at planar membrane surfaces. *J. Phys. Chem. B.* 104:863–868.

Lagerholm, B. C., T. E. Starr, Z. N. Volovyk, and N. L. Thompson. 2000. Rebinding of IgE Fabs at haptenated planar membranes: measurement by total internal reflection with fluorescence photobleaching recovery. *Biochemistry.* 39:2042–2051.

Magde, D., E. L. Elson, and W. W. Webb. 1974. Fluorescence correlation spectroscopy. II. An experimental realization. *Biopolymers.* 13:29–61.

McConnell, H. M., T. H. Watts, R. M. Weis, and A. A. Brian. 1986. Supported planar membranes in studies of cell–cell recognition in the immune system. *Biochim. Biophys. Acta.* 864:95–106.

Meseth, U., T. Wohland, R. Rigler, and H. Vogel. 1999. Resolution of fluorescence correlation measurements. *Biophys. J.* 76:1619–1631.

Moore, K. J., S. Turconi, S. Ashman, M. Ruediger, U. Haupts, V. Emerick, and A. J. Pope. 2000. Single molecule detection technologies in miniaturized high throughput screening: fluorescence correlation spectroscopy. *J. Biomol. Screen.* 4:335–353.

Müller, B., H.-G. Zerwes, K. Tangemann, J. Paeter, and J. Engel. 1993. Two-step binding mechanism of fibrinogen αIIbβ3 integrin reconstituted into planar lipid bilayers. *J. Biol. Chem.* 268:6800–6808.

Olofsson, B., M. Jeltsch, U. Eriksson, and K. Alitalo. 1999. Current biology of VEGF-B and VEGF-C. *Curr. Opin. Biotechnol.* 10:528–535.

Palmer, A. G., and N. L. Thompson. 1989a. Fluorescence correlation spectroscopy for detecting submicroscopic clusters of fluorescent molecules in membranes. *Chem. Phys. Lipids.* 50:253–270.

Palmer, A. G., and N. L. Thompson. 1989b. Optical spatial intensity profiles for high order autocorrelation in fluorescence spectroscopy. *App. Optics.* 28:1214–1220.

Pisarchick, M. L., and N. L. Thompson. 1990. Binding of a monoclonal antibody and its Fab fragment to supported phospholipid monolayers measured by total internal reflection fluorescence microscopy. *Biophys. J.* 58:1235–1249.

Ravetch, J. V. 1997. Fc receptors. *Curr. Opin. Immunol.* 9:121–125.

Sackmann, E. 1996. Supported membranes: scientific and practical applications. *Science.* 271:43–48.

Schuler, J., J. Frank, U. Trier, M. Schafer-Korting, and W. A. Saenger. 1999. Interaction kinetics of tetramethylrhodamine transferrin with human transferrin receptor studied by fluorescence correlation spectroscopy. *Biochemistry.* 38:8402–8408.

Schwille, P., S. Kummer, A. A. Heikal, W. E. Moerner, and W. W. Webb. 2000. Fluorescence correlation spectroscopy reveals fast optical excitation-driven intramolecular dynamics of yellow fluorescent proteins. *Proc. Natl. Acad. Sci. USA.* 97:151–156.

Seal, R. P., and S. G. Amara. 1999. Excitatory amino acid transporters: A family in flux. *Annu. Rev. Pharmacol. Toxicol.* 39:431–456.

Silverman, L., R. Campbell, and J. R. Broach. 1998. New assay technologies for high-throughput screening. *Curr. Opin. Chem. Biol.* 2:397–403.

Sterrer, S., and K. Henco. 1997. Fluorescence correlation spectroscopy (FCS)—A highly sensitive method to analyze drug/target interactions. *J. Recept. Signal Transduct. Res.* 17:511–520.

Tamm, L. K., and E. Kalb. 1993. Microspectrofluorometry on supported planar membranes. *In* Molecular Luminescence Spectroscopy: Methods and Applications Part 3, Wiley. 253–305.

Thompson, N. L. 1982. Surface binding kinetic rates of nonfluorescent molecules may be obtained by total internal reflection with fluorescence correlation spectroscopy. *Biophys. J.* 38:327–329.

Thompson, N. L. 1991. Fluorescence correlation spectroscopy. *In* Topics in Fluorescence Spectroscopy, Vol. 1. J. R. Lakowicz, editor. Plenum Press, New York. 337–378.

Thompson, N. L., and D. Axelrod. 1983. Immunoglobulin surface-binding kinetics studied by total internal reflection with fluorescence correlation spectroscopy. *Biophys. J.* 43:103–114.

Thompson, N. L., T. P. Burghardt, and D. Axelrod. 1981. Measuring surface dynamics of biomolecules by total internal reflection fluorescence with photobleaching recovery or correlation spectroscopy. *Biophys. J.* 33:435–454.

Thompson, N. L., and B. C. Lagerholm. 1997. Total internal reflection fluorescence: applications in cellular biophysics. *Curr. Opin. Biotechnol.* 8:58–64.

Thompson, N. L., K. H. Pearce, and H. V. Hsieh. 1993. Total internal reflection fluorescence microscopy: application to substrate-supported planar membranes. *Eur. Biophys. J.* 22:367–378.

Van Craenenbroeck, E., and Y. Engelborghs. 1999. Quantitative characterization of the binding of fluorescently labeled colchicine to tubulin in vitro using fluorescence correlation spectroscopy. *Biochemistry.* 38: 5082–5088.

Van Craenenbroeck, E., and Y. Engelborghs. 2000. Fluorescence correlation spectroscopy: molecular recognition at the single molecule level. *J. Mol. Recog.* 13:93–100.

Vanden Broek, W., Z. Huang, and N. L. Thompson. 1999. High order autocorrelation with imaging fluorescence correlation spectroscopy: application to IgE on supported planar membranes. *J. Fluoresc.* 9:313–324.

Winkler, T., U. Kettling, A. Koltermann, and M. Eigen. 1999. Confocal fluorescence coincidence analysis: an approach to ultra high-throughput screening. *Proc. Natl. Acad. Sci. USA.* 96:1375–1378.

Wiseman, P. W., and N. O. Petersen. 1999. Image correlation spectroscopy. II. Optimization for ultrasensitive detection of preexisting platelet-derived growth factor-beta receptor oligomers on intact cells. *Biophys. J.* 76:963–977.

Wohland, T., K. Friedrich, R. Hovius, and H. Vogel. 1999. Study of ligand–receptor interactions by fluorescence correlation spectroscopy with different fluorophores: evidence that the homopentameric 5-hydroxytryptamine type 3(As) receptor binds only one ligand. *Biochemistry.* 38:8671–8681.

Zwaal, R. F. A., P. Comfurius, and E. M. Bevers. 1998. Lipid–protein interactions in blood coagulation. *Biochim. Biophys. Acta Rev. Biomemb.* 1376:433–453.